タイトル Title	Enveloped artificial viral capsids self-assembled from anionic beta-annulus peptide and cationic lipid bilayer
著者 Auther(s)	Furukawa, Hiroto; Inaba, Hiroshi; Inoue, Fumihito; Sasaki, Yoshihiro; Akiyoshi, Kazunari; Matsuura, Kazunori
掲載誌・巻号・ページ Citation	CHEMICAL COMMUNICATIONS , 56 (52) : 7092 - 7095
刊行日 Issue Date	2020-07-04
資源タイプ Resource Type	学術雑誌論文 / Journal Article
版区分 Resource Version	著者版 / Author
権利 Rights	(C) The Royal Society of Chemistry 2020
DOI	10.1039/d0cc02622k
URL	https://repository.lib.tottori-u.ac.jp/9869

COMMUNICATION

Enveloped Artificial Viral Capsids Self-assembled from Anionic β-Annulus Peptide and Cationic Lipid Bilayer

Received 00th January 20xx,
Accepted 00th January 20xx

DOI: 10.1039/x0xx00000x

Hiroto Furukawa,[a] Hiroshi Inaba,[ab] Fumihito Inoue,[c] Yoshihiro Sasaki,[c] Kazunari Akiyoshi,[c] and Kazunori Matsuura*[ab]

Anionic artificial viral capsids were self-assembled from β-annulus-EE peptide, then complexed with lipid-bilayer-containing cationic lipids via electrostatic interaction to form enveloped artificial viral capsids. The critical aggregation concentration of the enveloped artificial viral capsid was significantly lower than that of the uncomplexed artificial viral capsid, indicating that the lipid bilayer stabilised the capsid structure.

Natural viruses are nano-sized supramolecular structures that replicate after invading a host cell. They form nucleocapsid structures of genomic nucleic acids covered with capsids self-assembled from proteins. In rod-shaped viruses such as the tobacco mosaic virus, the proteins assemble helically around the nucleic acids, and in spherical viruses such as the adenovirus and human papilloma virus, they form icosahedral symmetric capsids around the nucleic acids.[1] The nucleocapsid structures of envelope-type viruses such as influenza virus, human immunodeficiency virus and coronavirus are covered with lipid bilayers which embed membrane proteins. These bilayers are involved in various functions such as cell adhesion and material transport between cells.[2,3]

Over the past three decades, natural viral capsids and virus-like protein nanocapsules have attracted much attention as organic materials with discrete sizes, hollow interior nanospaces, unique morphologies and specific numbers of assembly units.[4-10] Virus-like capsids have been developed as nanocarriers of drug delivery systems (DDSs), nanotemplates and nanoreactors. Recently, artificial capsid-like nanostructures that mimic natural viral capsids have been developed by *de novo* design of self-assembling proteins.[11,12] However, a chemical strategy for constructing artificial enveloped virus-like structures has lagged behind this progress.[13] Artificial enveloped viral capsids would encapsulate drugs as novel DDS carriers equipped with various functional membrane proteins on the envelope. Furthermore, by artificially constructing the enveloped viral capsids, we might elucidate the detailed mechanism of viral infection of host cells.

Recent progress on *de novo* design of self-assembling peptides has enabled the construction of peptide-based viral capsids.[14-20] Previously, we demonstrated that 24-mer β-annulus peptides (INHVGGTGGAIMAPVAVTRQLVGS), which participate in forming the dodecahedral internal skeleton of tomato bushy stunt virus (TBSV),[21,22] spontaneously self-assemble into a hollow peptide nanocapsule (artificial viral capsid) with a size range of 30–50 nm in water.[17,18] This artificial viral capsid can encapsulate anionic dyes,[23] DNA,[24] and quantum dots[25] in its cationic interior. Furthermore, its exterior surface can be decorated with gold nanoparticles,[26] coiled-coil peptides,[27] single-stranded DNA,[28] human serum albumin,[29] and RNase S[30] by modifying the C-terminal of the β-annulus peptide which is directed toward the capsid exterior.

Nanostructures can also be covered with lipid bilayers to improve their stability and functionality.[31-34] For example, Kostarelos and co-workers reported that coating the spikes of adenovirus with cationic lipid improves their cell permeability.[32] Yanagisawa and co-workers demonstrated that a stable complex of a DNA nanostructure covered with cationic liposome via electrostatic interaction is resistant to osmotic shock.[34] In this paper, we develop a simple strategy for constructing enveloped artificial viral capsids through the self-assembly of β-annulus peptides. We demonstrate that electrostatic interaction between an artificial viral capsid with an anionic surface and a lipid-bilayer-containing cationic lipid (DOTAP/DOPC) forms a stable enveloped artificial viral capsid (Figure 1A).

The artificial viral capsid with its anionic surface forms the scaffold of the enveloped artificial viral capsid. To create the anionic surface, we noted that the C-terminal region of the β-annulus peptide points toward the outer surface of the artificial viral capsid,[23] and designed a 26-residue β-annulus peptide containing two glutamic acids at its C-terminal (INHVGGTGGAIMAPVAVTRQLVGSEE). The β-annulus-EE peptide was synthesised by standard Fmoc solid-phase chemistry, purified by reverse-phase HPLC, and confirmed by MALDI-TOF-MS (m/z = 2563 $[M]^+$, Figure S1 and S2). Dynamic light scattering (DLS) measurements of the β-Annulus-EE peptide (50 μM) in 10 mM Tris-HCl buffer (pH 7.0) revealed an assemblage with a size distribution of 67 ± 21 nm (Figure 1B). The size distributions of the β-annulus-EE peptide assemblies remained at 60−80 nm over a wide concentration range (10−250 μM; see Figure S3). Transmission

[a] *Department of Chemistry and Biotechnology, Graduate School of Engineering, Tottori University, Koyama-Minami 4-101, Tottori 680-8552, Japan. E-mail: ma2ra-k@tottori-u.ac.jp*
[b] *Centre for Research on Green Sustainable Chemistry, Tottori University, Koyama-Minami 4-101, Tottori 680-8552, Japan*
[c] *Department of Polymer Chemistry, Graduate School of Engineering, Kyoto University, Katsura, Nishikyo-ku, Kyoto 615-8510, Japan*
†Electronic Supplementary Information (ESI) available: Experimental details and supporting figures. See DOI: 10.1039/x0xx00000x

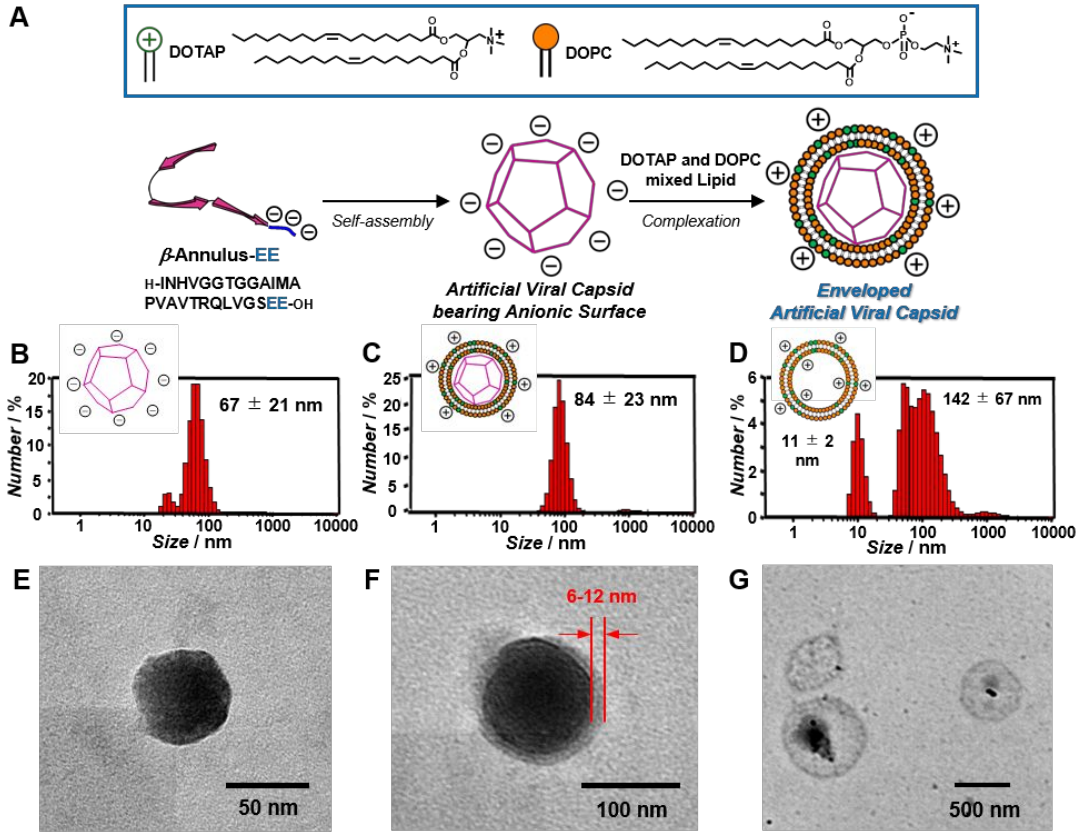

Fig. 1 (A) Schematic of constructing an enveloped artificial viral capsid via electrostatic interaction. (B–G) Size distributions obtained from dynamic light scattering and TEM images of (B, E) artificial viral capsid-bearing anionic surface (50 μM *β*-annulus-EE peptide), (C, F) enveloped artificial viral capsid (50 μM *β*-annulus-EE peptide, 150 μM DOTAP and 1500 μM DOPC) and (D, G) liposome (150 μM DOTAP and 1500 μM DOPC) in 10 mM Tris-HCl buffer (pH 7.0) at 25 °C. TEM samples were stained with EM stainer.

electron microscopy (TEM) also showed the formation of spherical assemblies with approximate diameters of 50 nm (Figure 1E). The ζ-potential of the *β*-annulus-EE peptide assemblies at pH 7.0 was −29 ± 7 mV (Figure S4, blue line), corresponding to an expected formal charge of −3 at the C-terminal region directed toward the outer capsid surface. These results indicate that the *β*-annulus-EE peptides self-assembled into an artificial viral capsid with an anionic surface. This assembly was slightly larger than the artificial viral capsid self-assembled from the typical *β*-annulus peptide of TBSV (30–50 nm).[18]

The enveloped artificial viral capsid was constructed by complexing the anionic artificial viral capsid with lipid-bilayer-containing cationic lipids by the hydration method. An aqueous solution of the anionic artificial viral capsid self-assembled from *β*-annulus-EE peptide (50 μM) was added to lipid film consisting of a 1:10 mixture of a cationic lipid (1,2-dioleoyl-3-trimethylammonium-propane: DOTAP) and a zwitterionic lipid (1,2-dioleoyl-*sn*-glycero-3-phosphocholine: DOPC). The cation/anion charge ratio of the complex was controlled at 1:1. Uncomplexed free liposomes were removed by ultracentrifugation. From DLS measurements, the size distribution of the complex was determined as 84 ± 23 nm (Figure 1C), slightly exceeding that of the anionic artificial viral capsid (67 ± 21 nm; see Figure 1B). The TEM image of the complex revealed deeply stained spherical structures of approximate diameter 100 nm, covered with thinly stained fringe structures of approximate thickness 6−12 nm (Figure 1F). The size distribution histogram of the complex obtained from the TEM images showed that the average diameter of spherical structures was 140 ± 20 nm (Figure S6), which is larger than that obtained from the DLS size distribution. The ζ-potential of the complex was 72 ± 10 mV, which is comparable to that of the DOTAP/DOPC (1:10) liposome: 75 ± 11 mV (Figure S4). As the estimated length of a lipid molecule is 5 nm, the thickness of the observed fringes was comparable to one or two lipid bilayers. Conversely, DLS measurements of the DOTAP/DOPC liposomes without the *β*-annulus-EE peptide showed multiple broad size distributions (Figure 1D), and the TEM image revealed the formation of capsule structures approximately 200–500 nm wide (Figure 1G). In addition, complexation of the anionic artificial viral capsid with DOPC alone (without DOTAP) afforded large aggregates with broad size distributions (Figure S8). These results confirmed that complexation of the anionic artificial viral capsid with DOTAP/DOPC lipid formed an artificial viral capsid with a cationic envelope. The complexation of the capsid with DOTAP alone showed broad bimodal size distribution and irregular spherical structures were observed by TEM (Figure S9), which might be caused by electrostatic repulsion among the cationic lipids. The enveloped artificial viral capsid could be constructed by the same hydration method with different ratio of DOTAP/DOPC (1:5), but DLS of the constructed enveloped artificial viral capsid showed relatively broad size distribution (Figure S11). These results indicate that optimal DOTAP/DOPC ratio (1:10) is indispensable for the formation of enveloped capsids (~80 nm) with narrow size distribution.

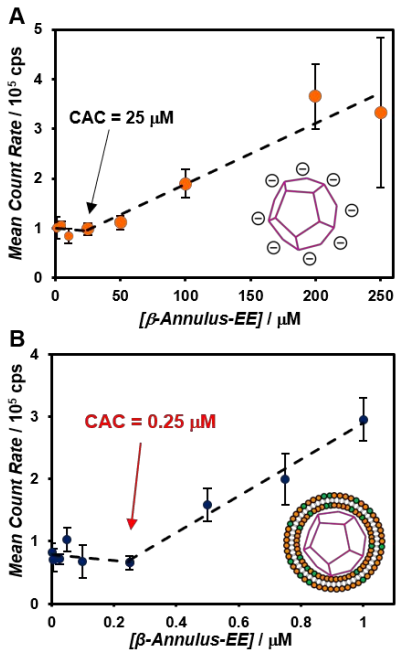

Fig. 2. Effect of peptide concentration on the scattering intensity at 25 °C: (A) the artificial viral capsid and (B) the enveloped artificial viral capsid.

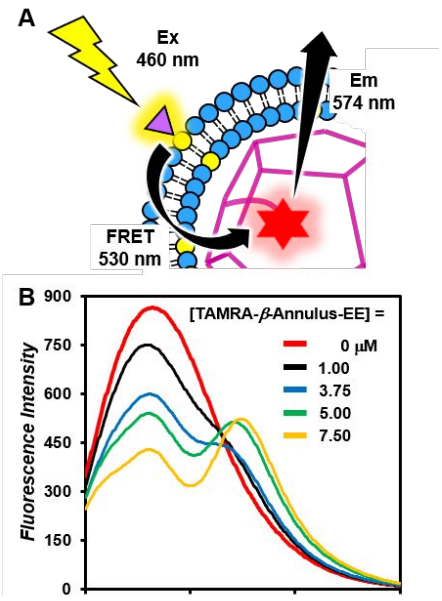

Fig. 3. (A) Schematic of FRET between TAMRA-β-annulus-EE and NBD-PE on the enveloped artificial viral capsid. (B) Fluorescence emission spectra of the NBD-PE (3.75 μM) and TAMRA-β-annulus-EE (0, 1.00, 3.75, 5.00, 7.50 μM) excited at 460 nm in 10 mM Tris-HCl buffer (pH 7.0) at 25 °C.

To evaluate the stabilisation effect of the lipid bilayer envelope on the artificial viral capsid, we determined the critical aggregation concentration (CAC) of the capsid. To this end, we measured the peptide-concentration dependence on the scattering intensity obtained from DLS measurements. The CAC of the anionic artificial viral capsid was determined as 25 μM (Figure 2A), comparable to that of the conventional artificial viral capsid without an anionic surface.[18] In contrast, the CAC of the enveloped artificial viral capsid was 0.25 μM (Figure 2B), indicating that β-annulus−EE peptide can form the enveloped complex at 100 times lower concentration in the lipid environment than in the no-lipid environment. The anionic artificial viral capsids maintained their size distribution for three days and were thereafter destabilised to form aggregates (Figure S13A), probably by electrostatic repulsion between the β-annulus-EE peptides. In contrast, the enveloped artificial viral capsid maintained the size distribution of about 100 nm for 16 days at least (Figure S13B). These results indicate that the artificial viral capsid self-assembled from β-annulus-EE peptide was electrostatically stabilised by complexing with the cationic lipid bilayer.

To further confirm the formation of the complex, a fluorescence-labelled enveloped viral capsid was constructed by complexing tetramethylrhodamine (TAMRA)-labelled anionic capsid with nitrobenzoxadiazole (NBD)-labelled lipid bilayer (Figure S14). TAMRA-labelled β-annulus-EE peptide was synthesised by conjugating β-annulus-EE peptide with a Cys residue at its N-terminal, which is directed toward the inside of the capsid, with TAMRA-maleimide (Figure S15, S16). When TAMRA-β-annulus-EE and β-annulus-EE peptide were co-assembled at a 1:49 ratio, TAMRA-modified capsids of approximate size 98 nm were obtained (Figure S17A). The TAMRA-modified capsids were mixed with lipid films of DOTAP/DOPC/NBD-PE (2/19/1) by the hydration method, yielding complexes of approximate size 144 nm (Figure S17B). If the donor NBD (excitation wavelength (Ex): 463 nm, emission wavelength (Em): 536 nm) and the acceptor TAMRA (Ex: 555 nm, Em: 580 nm) are in close proximity in the enveloped artificial viral capsid, fluorescence resonance energy transfer (FRET) should occur (Figure 3A). Figure 3B shows the fluorescence spectral change when the NBD on the enveloped capsid was excited in the presence of different concentration of TAMRA-β-annulus-EE. Increasing the concentration of TAMRA-β-annulus-EE peptide significantly reduced the fluorescence intensity derived from the donor NBD, and increased the fluorescence intensity from the acceptor TAMRA. From the fluorescence intensity ratio of the donor, the FRET efficiency was estimated as ~0.50 and the average distance between the donor and acceptor was calculated as 5.1 nm, comparable to the thickness of one lipid bilayer (5−6 nm).

The distributions of the individual fluorescence intensities derived from TAMRA and NBD on the enveloped viral capsid were measured by imaging flow cytometry of 10,000 particles. The TAMRA-labelled artificial viral capsid yielded a relatively broad distribution of TAMRA fluorescence intensities (Figure 4A), whereas the liposome containing NBD-PE obtained a relatively broad distribution of NBD fluorescence intensities (Figure 4B). Meanwhile, the TAMRA/NBD-labelled enveloped artificial viral capsid showed a broad fluorescence intensity distribution derived from both TAMRA and NBD (Figure 4C). These FRET and flow cytometry results further clarified the co-existence of β-annulus-EE peptide and lipid bilayer on the enveloped artificial viral capsids.

In conclusion, we successfully constructed an enveloped artificial viral capsid by complexing an anionic artificial viral capsid self-assembled from the β-annulus-EE peptide with cationic lipid bilayers. The DLS, TEM, and ζ-potential measurements revealed the formation of enveloped artificial viral capsids with a size distribution of 80−100

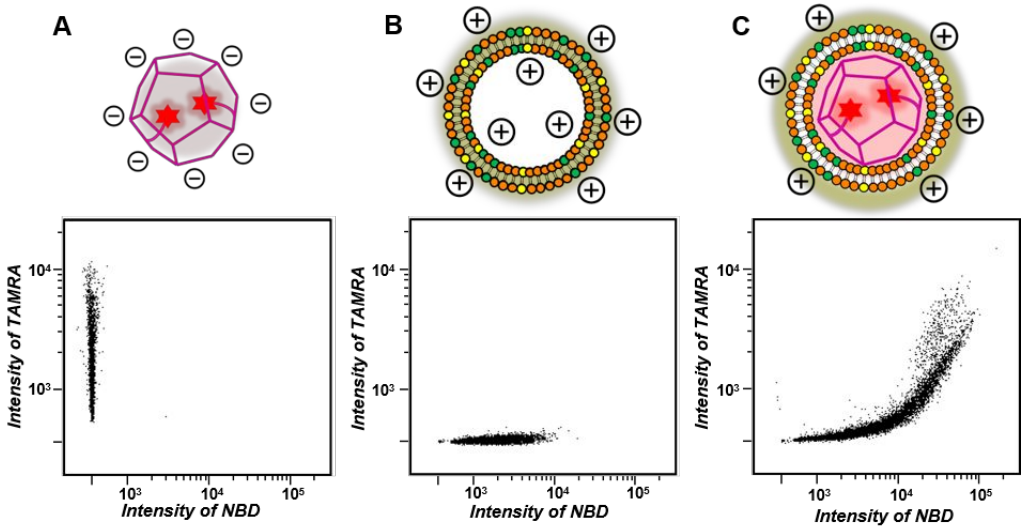

Fig. 4. Flow cytometry analyses of (A) TAMRA-labelled encapsulated artificial viral capsid (1 μM TAMRA-β-annulus-EE, 49 μM β-annulus-EE peptide), (B) NBD-labelled liposome (150 μM DOTAP, 1425 μM DOPC, 75 μM NBD-PE), (C) TAMRA/NBD-labelled enveloped artificial viral capsid (1 μM TAMRA-β-annulus-EE, 75 μM NBD-PE).

nm. The enveloped viral capsids were further confirmed by the FRET and imaging flow cytometry analyses. Interestingly, the enveloped artificial viral capsid was formed at 100-times lower peptide concentration than the anionic artificial viral capsid. We envisage the use of the stable enveloped artificial viral capsid as a platform for displaying unstable proteins on the capsid surface and embedding membrane proteins on the envelope. These would be applied for novel DDS carriers, artificial vaccines and model systems of viral infection.

Conflicts of interest

There are no conflicts to declare.

Acknowledgements

This research was supported by Grand-in-Aid for Scientific Research (B) (JSPS KAKENHI Grand No. JP18H02089). The author would like to thank MARUZEN-YUSHODO Co., Ltd. For the English language editing.

Notes and references

1 *Structure and Physics of Viruses*, M. G. Mateu (Ed.), Springer, 2013.
2 M. Marsh, *Biochem. J*., 1984, **218**, 1.
3 B. J. Chen, R. A. Lamb, *Virology*, 2008, **372**, 221.
4 *Viral Nanotechnology*, Y. Khudyakov, P. Pumpens (Ed.), CRC Press, 2016.
5 N. F. Steinmetz, D. J. Evans, *Org. Biomol. Chem*., 2007, ***5***, 2891.
6 T. Douglas, M. Young, *Science*, 2006, **312**, 873.
7 D. Papapostolou, S. Howorka, *Mol. BioSyst*., 2009, **5**, 723.
8 L. S. Witus, M. B. Francis, *Acc. Chem. Res*., 2011, **44**, 774.
9 L. M. Bronstein, *Small*, 2011, **7**, 1609.
10 Y. Azuma, T. G. W. Edwardson, D. Hilvert, *Chem. Soc. Rev*., 2018, **47**, 3543.
11 Y. T. Lai, E. Reading, G. L. Hura, K. L. Tsai, A. Laganowsky, F. J. Asturias, J. A. Tainer, C. V. Robinson, T. O. Yeates, *Nat. Chem*., 2014, **6**, 1065.
12 Y. Hsia, J. B. Bale, S. Gonen, D. Shi, W. Sheffler, K. K. Fong, U. Nattermann, C. Xu, P. S. Huang, R. Ravichandran, S. Yi, T. N. Davis, T. Gonen, N. P. King, D. Baker, *Nature*, 2016, **535**, 136.
13 J. Votteler, C. Ogohara, S. Yi, Y. Hsia, U. Nattermann, D. M. Belnap N. P. King, W. I. Sundquist, *Nature*, 2016, **540**, 292.
14 K. Matsuurua, *RSC Adv*., 2014, **4**, 2942.
15 B. E. I. Ramakers, J. C. M. van Hest, D. W. P. M. Löwik, *Chem. Soc. Rev*., 2014, **43**, 2743.
16 S. Lou, X. Wang, Z. Yu, L. Shi, *Adv. Sci*., 2019, **6**, 1802043.
17 K. Matsuura, *Chem. Commun*., 2018, **54**, 8944.
18 K. Matsuura, K. Watanabe, K. Sakurai, T. Matsuzaki, N. Kimizuka, *Angew. Chem., Int. Ed*., 2010, **49**, 9662.
19 E. De Santis, H. Alkassem, B. Lamarre, N. Faruqui, A. Bella, J. E. Noble, N. Micale, S. Ray, J. R. Burns, A. R. Yon, B. W. Hoogenboon, M. G. Ryadnoy, *Nat. Commun*., 2017, **8**, 2263.
20 I. E. Kepiro, I. Marzuoli, K. Hammond, X. Ba, H. Lewis, M. Shaw, S. B. Gunnoo, E. De Santis, U. Ł apińska, S. Pagliara, M. A. Holmes, C. D. Lorenz, B. M. Hoogenboom, F. Fraternali, M. G. Ryadnov, *ACS Nano*, 2020, **14**, 1609.
21 A. J. Olson, G. Bricogne, S. C. Harrison, *J. Mol. Biol*., 1983, **171**, 61.
22 P. Hopper, S. C. Harrison, R. T. Sauer, *J. Mol. Biol*., 1984, **177**, 701.
23 K. Matsuura, K. Watanabe, Y. Matsushita, N. Kimizuka, *Polym. J*., 2013, **45**, 529.
24 Y. Nakamura, H. Inaba, K. Matsuura, *Chem. Lett*., 2019, **48**, 544.
25 S. Fujita, K. Matsuura, *Chem. Lett*., 2016, **45**, 922.
26 K. Matsuura, G. Ueno, S. Fujita, *Polym. J*., 2015, **47**, 146.
27 S. Fujita, K. Matsuura, *Org. Biomol. Chem*., 2017, **15**, 5070.
28 Y. Nakamura, S. Yamada, S. Nishikawa, K. Matsuura, *J. Pept. Sci*., 2017, **23**, 636.
29 K. Matsuura, T. Honjo, *Bioconj. Chem*., 2019, **30**, 1636.
30 K. Matsuura, J. Ota, S. Fujita, Y. Shiomi, H. Inaba, *J. Org. Chem*., 2019, **85**, 1668.
31 C. M. A. Journot, V. Ramakrishna, M. I. Wallace, A. J. Turberfield, *ACS Nano*, 2019, **13**, 9973.
32 R. Singh, K. T. Al-Jamal, L. Lacerda, K. Kostarelos, *ACS Nano*, 2008, **2**, 1040.
33 S. D. Perrault, W. M. Shih, *ACS Nano*, 2014, **8**, 5132.
34 C. Kurokawa, K. Fujiwara, M. Morita, I. Kawamata, Y. Kawagishi, A. Sakai, Y. Murayama, S. Nomura, S. Murata, M. Takinoue, M. Yanagisawa, *PNAS*, 2017, **114**, 7228.

Supporting Information

Enveloped Artificial Viral Capsid Self-assembled from Anionic β-Annulus Peptide and Cationic Lipid Bilayer

Hiroto Furukawa,[a] Hiroshi Inaba,[ab] Fumihito Inoue,[c] Yoshihiro Sasaki,[c] Kazunari Akiyoshi,[c] and Kazunori Matsuura*[ab]

[a] Department of Chemistry and Biotechnology, Graduate School of Engineering, Tottori University, Koyama-Minami 4-101, Tottori 680-8552, Japan

[b] Centre for Research on Green Sustainable Chemistry, Tottori University, Koyama-Minami 4-101, Tottori 680-8552, Japan

[c] Department of Polymer Chemistry, Graduate School of Engineering, Kyoto University, Katsura, Nishikyo-ku,Kyoto 615-8510, Japan

EXPERMENTAL SECTION

General. Reversed-phase HPLC was performed at ambient temperature using Shimadzu LC-6AD liquid chromatography system equipped with a UV/vis detector (220 nm, Shimadzu SPD-10AVvp) and Inertsil WP300 C18 (GL Science) column (250 × 4.6 mm and 250 × 20 mm). MALDI-TOF mass spectra were obtained using an Autoflex-T2 instrument (Bruker Daltonics) in linear/positive mode with α-cyano-4-hydroxy cinnamic acid (α-CHCA) as a matrix. Deionized water of high resistivity (>18 MΩ cm) was purified using a Millipore Purification System (Milli-Q water) and was used as a solvent for the present peptides. Reagents were obtained from commercial sources and used without further purification.

Synthesis of β-Annulus-EE Peptide. The peptide H-Ile-Asn(Trt)-His(Trt)-Val-Gly-Gly-Thr(tBu)-Gly-Gly-Ala-Ile-Met-Ala-Pro-Val-Ala-Val-Thr(tBu)-Arg(Pbf)-Gln(Trt)-Leu-Val-Gly-Ser(tBu)-Glu(OtBu)-Glu(OtBu)-Alco-PEG resin was synthesized on Fmoc-Glu(OtBu)-Alko-PEG resin (494 mg, 0.123 mmol/g; Watanabe Chemical Ind. Ltd.) using Fmoc-based coupling reactions (4 equiv of Fmoc amino acid). *N*-methylpyrrolidone (NMP) solution containing (1-cyano-2-ethoxy-2-oxoethylidenaminooxy) dimethylamino-morpholino-carbenium hexafluorophosphate (COMU) and diisopropylamine was used as the coupling reagent. Fmoc deprotection was achieved using 20% piperidine in *N*,*N*-dimethylformamide (DMF). Progression of the coupling reaction and Fmoc deprotection was confirmed by TNBS and chloranil test kit (Tokyo Chemical Industry Co., Ltd.). Peptidyl-resins were washed with NMP and were then dried under a vacuum. Peptides were deprotected and cleaved from the resin by treatment with a cocktail of trifluoroacetic acid (TFA)/1,2-ethanedithiol/triisopropylsilane/water = 3.76/0.1/0.04/0.1 (mL) at room temperature for 4 h. Reaction mixtures were filtered to remove resins, and filtrates were concentrated in vacuo. The peptide was precipitated by adding methyl *tert*-butyl ether (MTBE) to the residue and the supernatant was decanted. After three times of repetitive washing with MTBE, precipitated peptide was dried in vacuo. The crude product was purified by reverse-phase HPLC eluting with a linear gradient of CH_3CN/water containing 0.1% TFA (5/95 to 100/0 over 100 min). The fraction containing the desired peptide was lyophilized to give 33.5 mg of a flocculent solid (35% yield). MALDI-TOF MS (matrix: α-CHCA): *m/z* = 2563 $[M]^+$.

Synthesis of TAMRA-β-Annulus-EE Peptide. β-Annulus-EE peptide bearing Cys at the N-terminal (CINHVGGTGGAIMAPVAVTRQLVGSEE) was synthesized on Fmoc-Glu(OtBu)-Alko-PEG resin (400 mg, 0.1 mmol/g; Watanabe Chemical Ind. Ltd.) by almost the same procedure described above. The crude product was purified by reverse-phase HPLC eluting with a linear gradient of CH_3CN/water containing 0.1% TFA (5/95 to 100/0 over 100 min). The fraction containing the desired peptide was lyophilized to give 7.4 mg of a flocculent solid (29% yield). MALDI-TOF MS (matrix: α-CHCA): *m/z* = 2667 $[M]^+$. The obtained Cys-β-annulus-EE peptide powder was dissolved in 20 mM sodium phosphate buffer (926 μL, pH 7.0) in an Eppendorf tube. Then, 38 mM tris(2-carboxyethyl)phosphine

hydrochloride (TCEP-HCl, Wako Co., Ltd.) in Milli-Q water (26 μL) and 10.4 mM tetramethylrhodamine-5-maleimide (TAMRA-maleimide, Funakoshi Co., Ltd.) in dimethyl sulfoxide (48 μL) were added the solution, and then the mixture was incubated in the dark at 25 °C for 7 h (final concentration: 250 μM Cys-*β*-annulus-EE peptide, 1 mM TCEP-HCl, 500 μM TAMRA-maleimide). After dialysis (Spectra/por7, cutoff Mw 1,000, Spectrum Laboratories, Inc.) in water for 24 h, the sample was purified by reverse-phase HPLC eluting with a linear gradient of CH_3CN/water containing 0.1% TFA (5/95 to 100/0 over 100 min). The fraction containing the desired peptide was lyophilized and dissolved in water (100 μL) to give an aqueous solution of 129 μM TAMRA-*β*-annulus-EE (5.2% yield). MALDI-TOF MS (matrix: *α*-CHCA): *m/z* = 3148 $[M]^+$.

Complexation of β-Annulus-EE Peptide with DOTAP/DOPC Lipids. Stock solution of 10 mM 1,2-dioleoyl-3-trimethylammonium-propane (DOTAP, Avanti Polar Lipids) in chloroform (3 μL), stock solution of 10 mM 1,2-dioleoyl-*sn*-glycero-3-phosphocholine (DOPC, Tokyo Chemical Industry Co., Ltd.) in chloroform (66 μL), methanol (33 μL) and chloroform (66 μL) were put in a glass tube and dried in vacuo for 6 h. The resulting lipid film was hydrated with solution of *β*-annulus-EE peptide solution (200 μL) in 10 mM Tris-HCl buffer (pH7.0) at 50 °C for 1 h, in which the cation / anion charge ratio of the complex was controlled to be 1: 1. Free liposomes were removed from the complex by ultracentrifugation using Optima MAX-TL Ultracentrifuge (25,000 rpm, 2 min, Beckman Coulter, Inc.). Figure S12 shows size distributions obtained from DLS and ζ-potential of enveloped artificial viral capsid immediately after complexing of *β*-annulus-EE peptide with DOTAP/DOPC (before equilibration for 1 h). The DLS showed multiple size distribution broader than that of the enveloped artificial viral capsid after incubation for 1 h (Figure 1C, 84 ± 23 nm). Therefore, incubation for 1 h after complexing plays an important role in equilibrating into stable and uniform enveloped artificial viral capsid.

Dynamic Light Scattering and ζ-Potential. Dynamic Light Scattering (DLS) of anionic artificial viral capsids, enveloped artificial viral capsids, and liposomes in 10 mM Tris-HCl buffer (pH 7.0) were measured at 25 °C using Zetasizer Nano ZS (MALVERN) with an incident He-Ne laser (633 nm) and ZEN2112-Low volume glass cuvette cell. During measurements, count rates (sample scattering intensities) were also provided. Correlation times of the scattered light intensities $G(\tau)$ were measured several times and there means were calculated for the diffusion coefficient. Hydrodynamic diameters of scattering particles were calculated using the Stokes-Einstein equation. ζ-Potentials of anionic artificial viral capsids, enveloped artificial viral capsids, and liposomes were measured at 25 °C using a Zetasizer Nano ZS with a DTS1070 clear disposable zeta cell.

Transmission Electron Microscopy. Aliquots (5 μL) of the DLS samples were applied to hydrophilized carbon-coated Cu-grids (C-SMART Hydrophilic TEM grids, ALLANCE Biosystems) for 1 min and then removed Subsequently, the TEM grids were instilled in the staining solution, 25% EM stainer aqueous solution (Nisshin EM Co., Ltd., 5 μL), for 15 min and then removed. After the

sample-loaded grids were dried in vacuo, they were observed by TEM (JEOL JEM 1400 Plus), using an accelerating voltage of 80 kV.

Imaging Flow Cytometry. Stock solution of 10 mM DOTAP (Avanti Polar Lipids) in chloroform (3 μL), stock solution of 10 mM DOPC (Tokyo Chemical Industry Co., Ltd.) in chloroform (28 μL), stock solution of 1 mM 1,2-dioleoyl-*sn*-glycero-3-phosphoethanolamine-*N*-(7-nitro-2-1,3-benzoxadiazol-4-yl) (NBD-PE, Avanti Polar Lipids) in chloroform (15 μL), methanol (23 μL) and chloroform (46 μL) were put in a glass tube and dried in vacuo for 6 h. The resulting lipid film was hydrated with solution (200 μL) of 49 μM *β*-annulus-EE + 1 μM TAMRA-*β*-annulus-EE peptide in 10 mM Tris-HCl buffer (pH7.0) at 50 °C for 1 h (final concentration: 49 μM *β*-annulus-EE, 1 μM TAMRA-*β*-annulus-EE, 150 μM DOTAP, 1425 μM DOPC, 75 μM NBD-PE), in which the cation / anion charge ratio of the complex controlled to be 1: 1. Free liposomes were removed from the complex by ultracentrifugation using Optima MAX-TL Ultracentrifuge (25,000 rpm, 2 min, Beckman Coulter, Inc.). The sample (200 μL) was observed by Imaging Flow Cytometer (Amnis FlowSight, Luminex Co., Ltd.) using an excitation laser (488 nm). The fluorescence intensity of 10,000 particles were analyzed by using software IDEAS (Luminex Co., Ltd.).

Fluorescence Resonance Energy Transfer (FRET). The enveloped artificial viral capsid labelled with NBD-PE (3.75 μM, 2.00 μM) as donor and TAMRA-*β*-annulus peptide (0−7.50 μM) as acceptor was constructed. The total concentration of unlabeled *β*-annulus-EE and TAMRA-*β*-annulus-EE were kept constant (50 μM). The fluorescence emission spectra (500-650 nm) exited at 460 nm of the samples was measured at 25°C by Jasco FP 8200 fluorescence spectrometer (JASCO Co., Ltd.) under temperature control using a Low Temp Bath BB301 (Yamato Scientific Co., Ltd.). The FRET efficiency *E* was calculated by using eq (1) [1]

$$E = 1 - \frac{I_{DA}}{I_D} \quad \cdot \cdot \cdot (1)$$

where I_D and I_{DA} are the fluorescence intensity of the donor in the absence and presence of the acceptor, respectively. The distance *R* between the donor and acceptor was calculated by using eq (2) [2]

$$R = R_0 \sqrt[6]{\frac{1-E}{E}} \quad \cdot \cdot \cdot (2)$$

where R_0 is Förster radius of the NBD/TAMRA-pair. It was set to R_0 = 5.1 nm according to the literature.[3]

Supporting figures

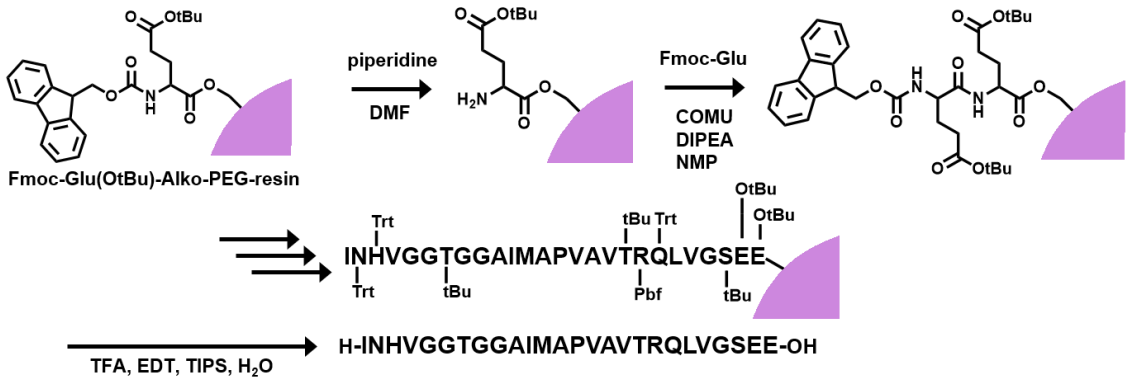

Figure S1. Synthesis of β-annulus-EE peptide by solid-phase Fmoc-chemistry.

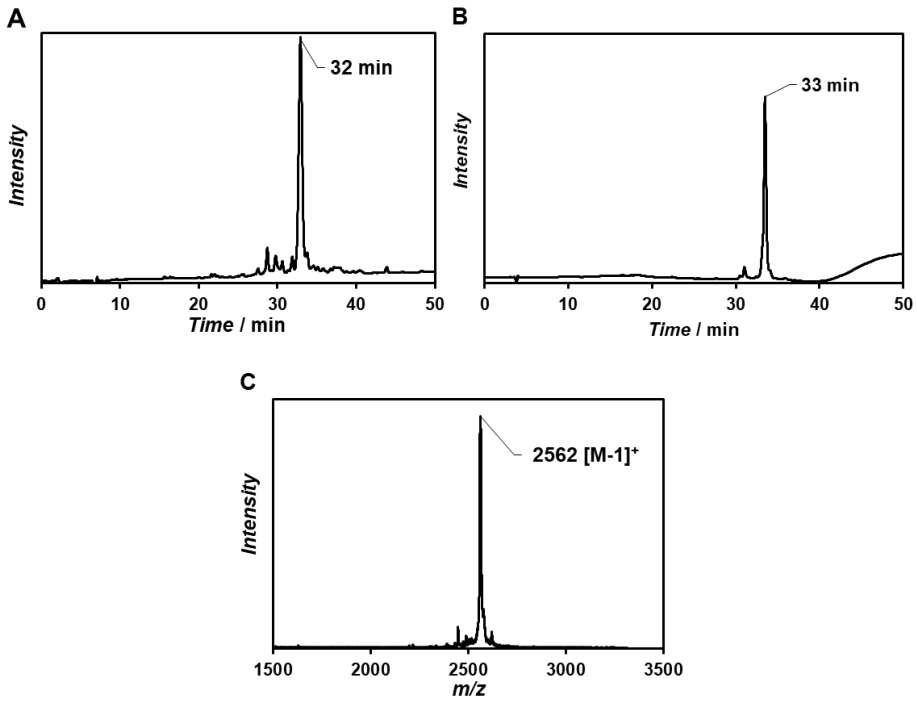

Figure S2. Reversed-phase HPLC chart of crude (A) and purified (B) β-annulus-EE peptide eluted with a linear gradient of CH_3CN/water containing 0.1% TFA (5/95 to 100/0 over 100 min), and MALDI-TOF-MS (C).

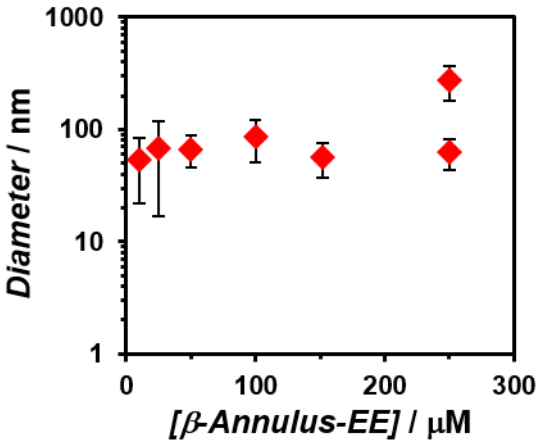

Figure S3. Concentration dependence of the size distribution obtained from DLS of *β*-annulus-EE peptide in 10 mM Tris-HCl buffer (pH 7.0) at 25 ºC.

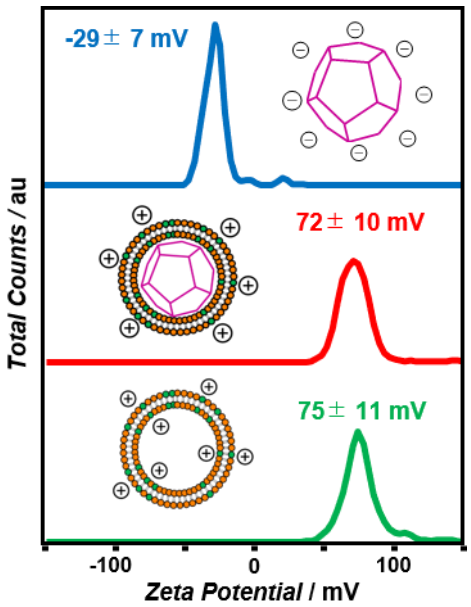

Figure S4. ζ-Potential of the artificial viral capsid bearing anionic surface (50 μM *β*-annulus-EE peptide, blue), enveloped viral capsid (50 μM *β*-annulus-EE peptide, 150 μM DOTAP and 1500 μM DOPC, red), liposome (150 μM DOTAP and 1500 μM DOPC, green) in 10 mM Tris-HCl buffer (pH 7.0) at 25 ºC.

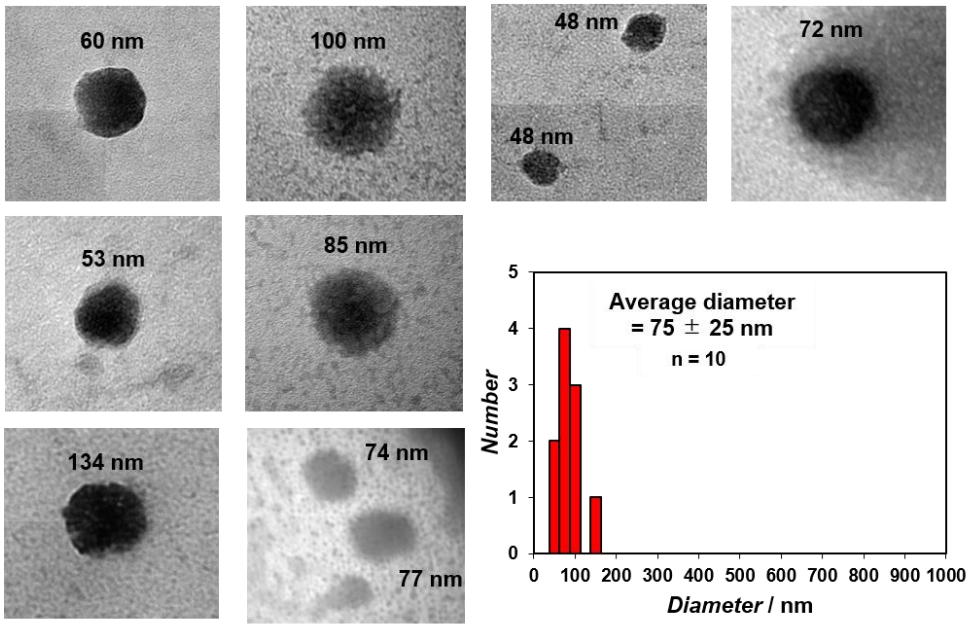

Figure S5. TEM images of the artificial viral capsid bearing anionic surface (50 μM *β*-annulus-EE peptide) and the size distribution.

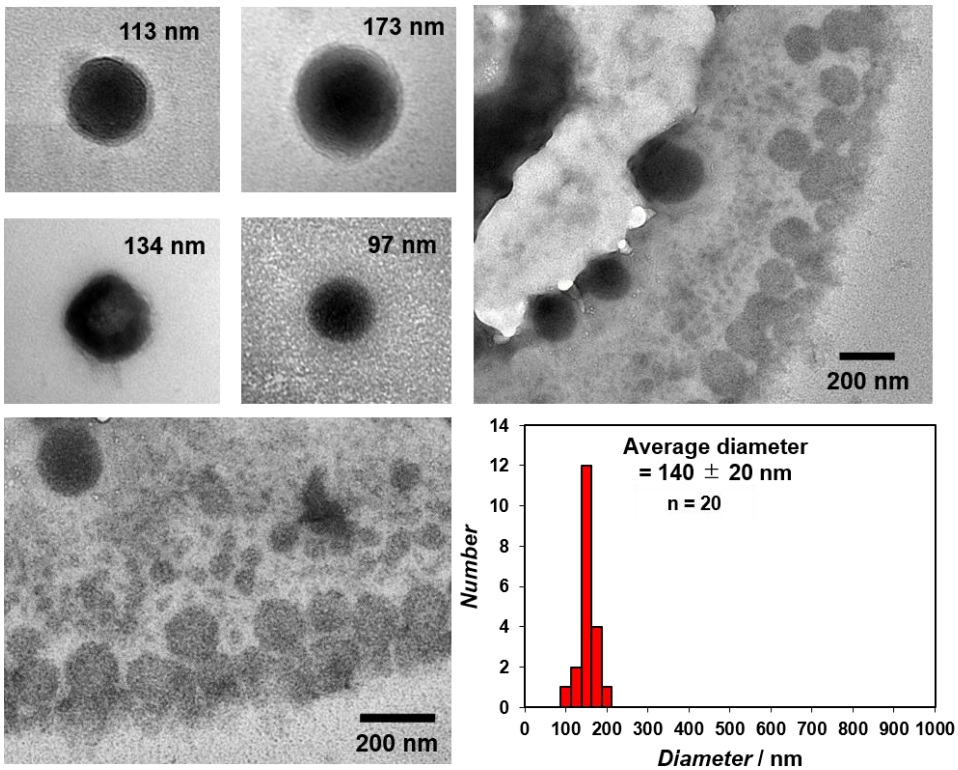

Figure S6. TEM images of enveloped artificial viral capsid (50 μM *β*-annulus-EE peptide, 150 μM DOTAP and 1500 μM DOPC) and the size distribution.

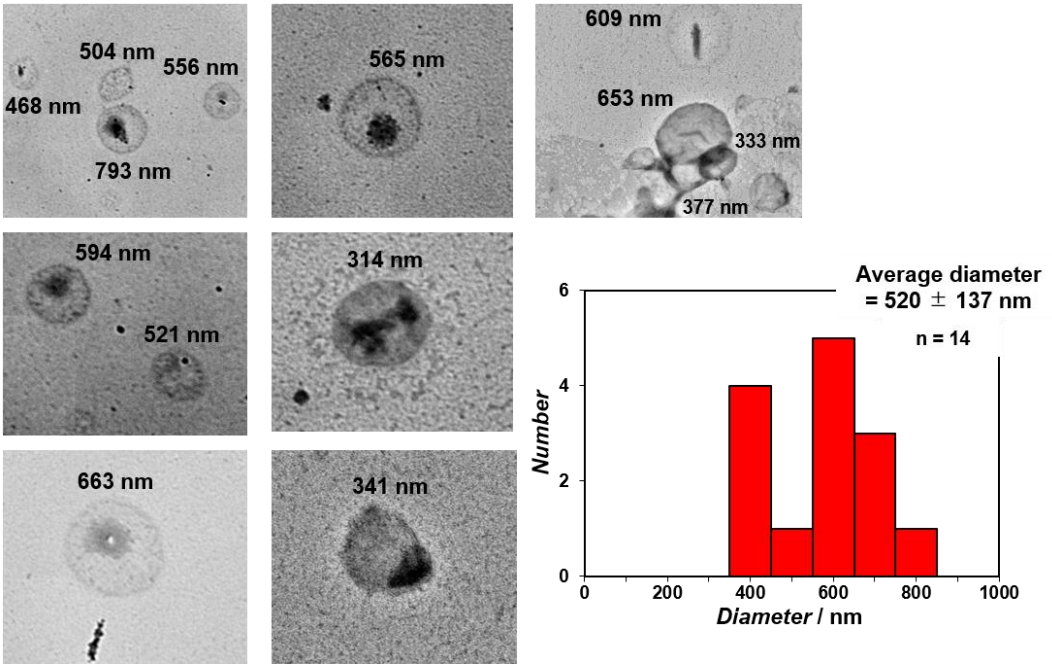

Figure S7. TEM images of liposome (150 μM DOTAP and 1500 μM DOPC) and the size distribution.

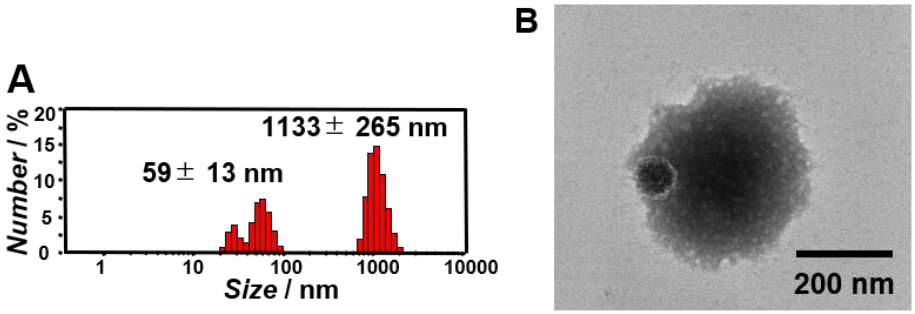

Figure S8. Size distribution obtained from DLS (A) and TEM image (B) of complex of anionic artificial viral capsid (50 μM *β*-annulus-EE peptide) with 1650 μM DOPC in 10 mM Tris-HCl buffer (pH 7.0) at 25 ºC. TEM sample was stained with sodium phosphotungstate.

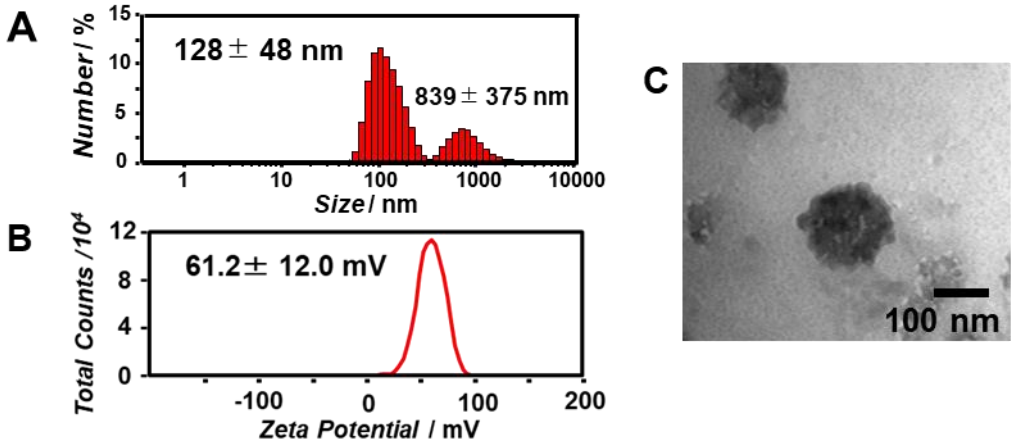

Figure S9. Size distributions obtained from DLS, ζ-potential and TEM image of enveloped artificial viral capsid complexing of 100 μM *β*-annulus-EE peptide with 300 μM DOTAP in 10 mM Tris-HCl buffer (pH 7.0) at 25 ºC.

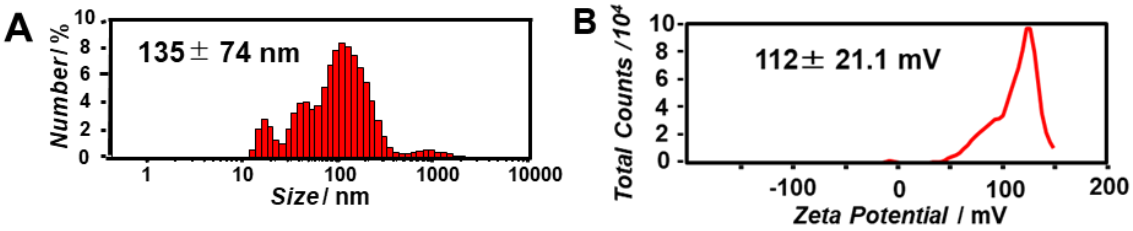

Figure S10. Size distribution obtained from DLS (A) and ζ-potential (B) of liposome consisting of 300 μM DOTAP in 10 mM Tris-HCl buffer (pH 7.0) at 25 ºC.

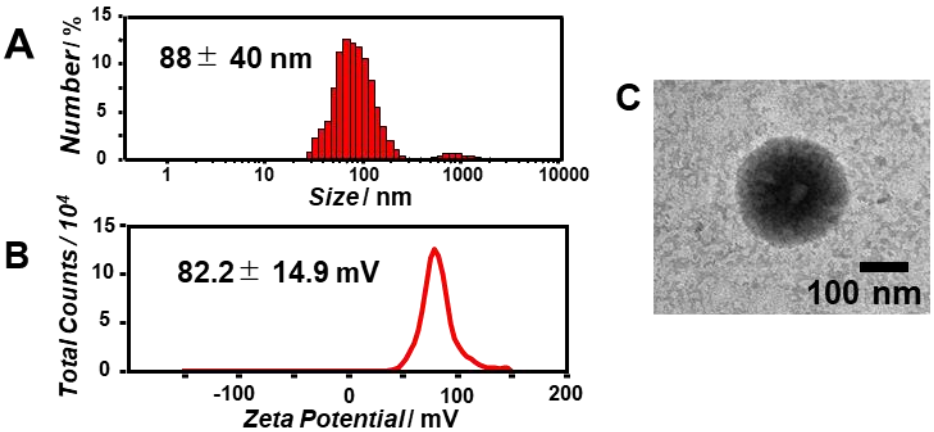

Figure S11. Size distribution obtained from DLS(A), ζ-potential (B) and TEM image (C) of enveloped artificial viral capsid consisting of 50 μM *β*-annulus-EE peptide, 150 μM DOTAP and 750 μM DOPC in 10 mM Tris-HCl buffer (pH 7.0) at 25 ºC.

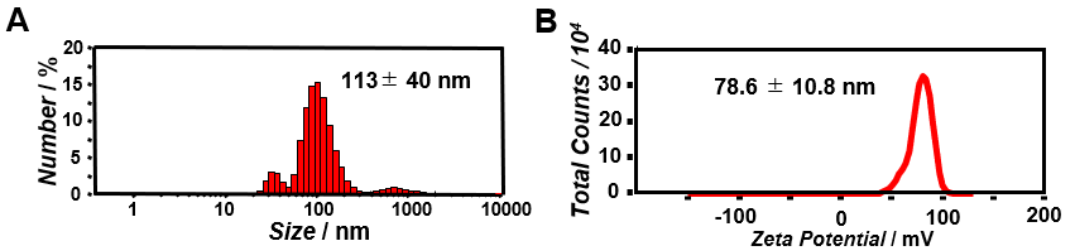

Figure S12. Size distributions obtained from DLS (A) and ζ-potential (B) of enveloped artificial viral capsid immediately after complexing of 50 μM *β*-annulus-EE peptide with 150 μM DOTAP and 1500 μM DOPC (before equilibration) in 10 mM Tris-HCl buffer (pH 7.0) at 25 ºC.

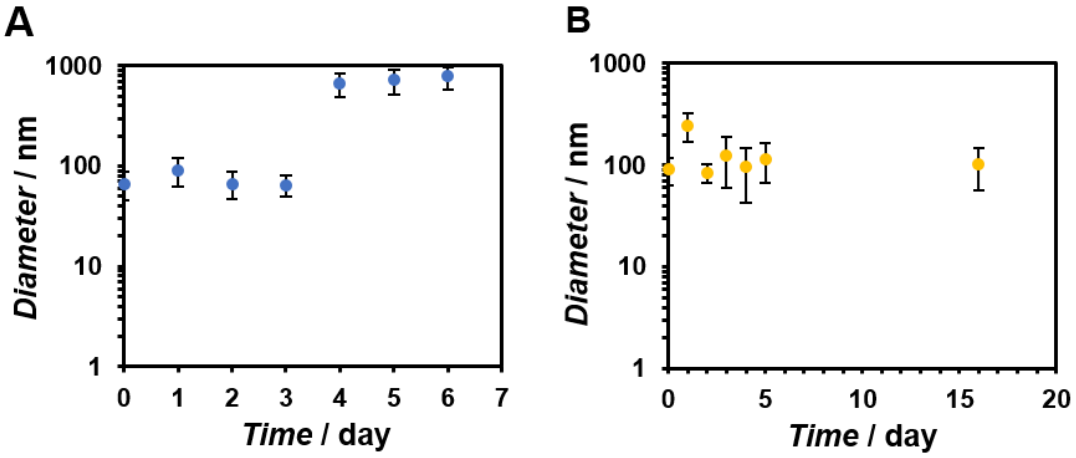

Figure S13. Time course of the size distribution of (A) 50 μM *β*-annulus-EE peptide and (B) enveloped artificial viral capsid ([*β*-annulus-EE] = 50 μM, [DOTAP] = 150 μM and [DOPC] = 1500 μM) in 10 mM Tris-HCl buffer (pH 7.0) at 25 ºC.

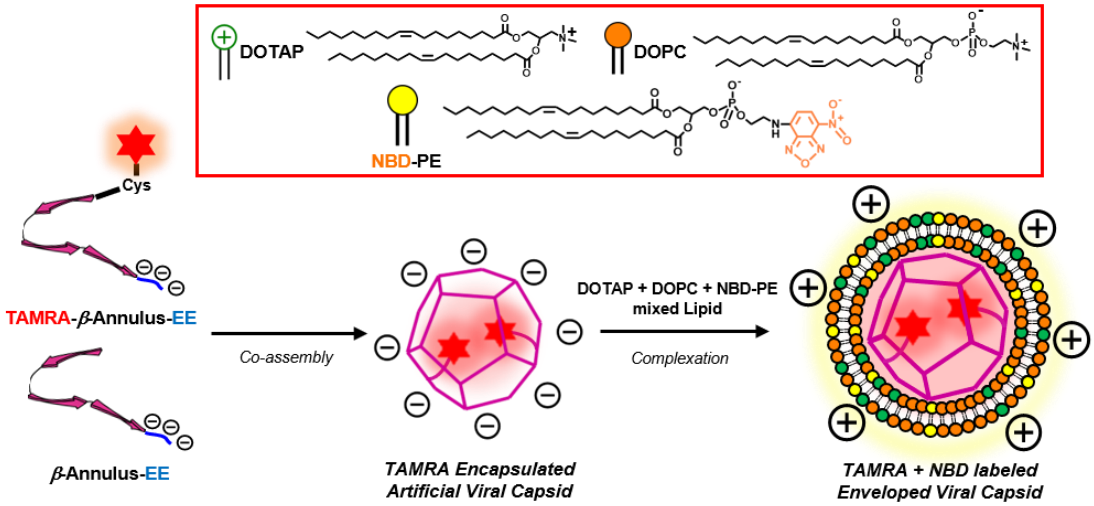

Figure S14. Schematic illustration of the construction of TAMRA/NBD-labelled enveloped artificial viral capsid.

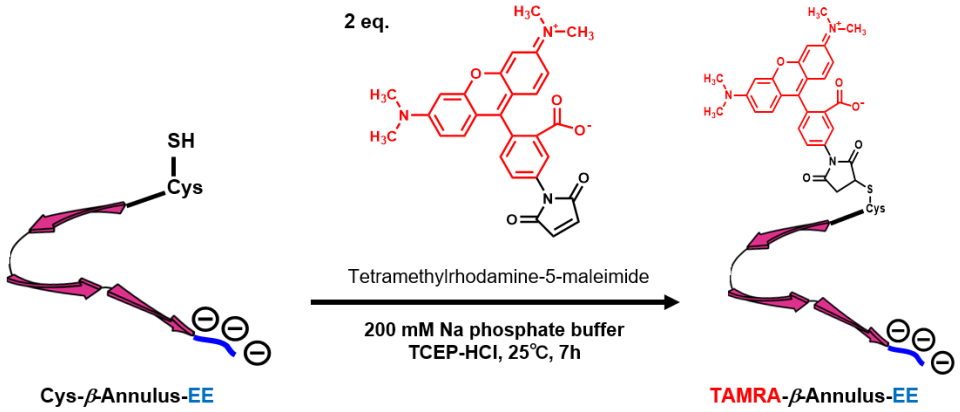

Figure S15. Synthesis of TAMRA-*β*-annulus-EE peptide.

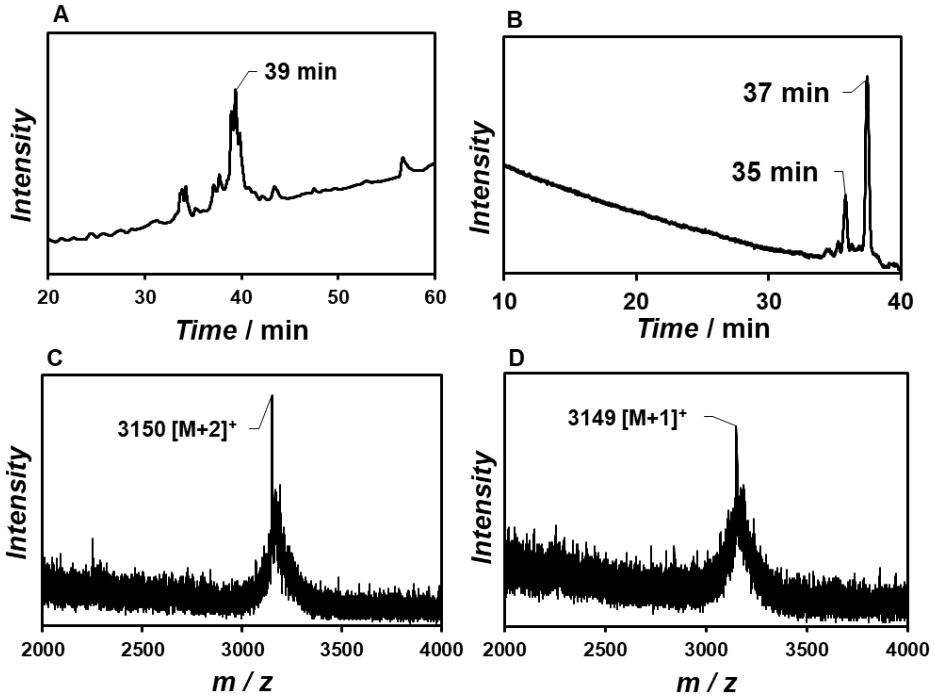

Figure S16. Reversed-phase HPLC chart of crude (A) and purified (B) TAMRA-*β*-annulus-EE peptide eluted with a linear gradient of CH_3CN/water containing 0.1% TFA (5/95 to 100/0 over 100 min), and MALDI-TOF-MS of peaks at 35 min (C) and 37 min (D). The two peaks at 35 and 37 min in chart (B) might be caused by equilibrium of opened-closed from of spirolactone ring of TAMRA.

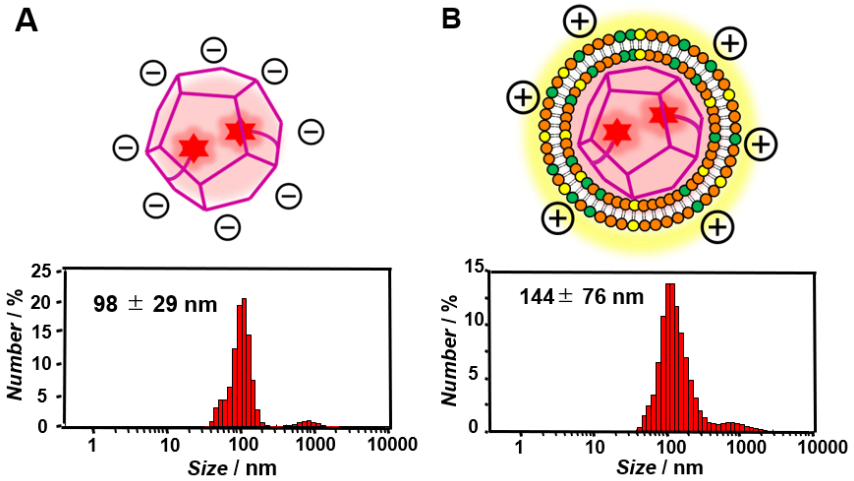

Figure S17. Size distributions obtained from DLS for (A) TAMRA-labelled artificial viral capsid (1 μM TAMRA-*β*-annulus-EE, 49 μM *β*-annulus-EE peptide), (B) TAMRA/NBD-labelled enveloped artificial viral capsid (1 μM TAMRA-*β*-annulus-EE, 49 μM *β*-annulus-EE peptide, 150 μM DOTAP, 1425 μM DOPC, 75 μM NBD-PE) in 10 mM Tris-HCl buffer (pH 7.0) at 25 ºC.

References

(1) *Principles of Fluorescence Spectroscopy*, J. R. Lakowicz, 3rd Ed. Springer, 2006.

(2) *Molecular Fluorescence: Principles and Applications*, B. Valeur, 2nd Ed. Wiley-VCH, 2012.

(3) P. E. Schneggenburger, S. Mullar, B. Worbs, C. Steinem, U. Diederrichsen, *J. Am. Chem. Soc*., 2010, **132**, 8020.

Table of contents entry

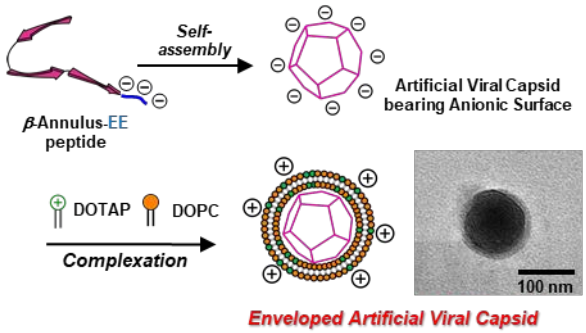

We demonstrated a simple strategy for constructing enveloped artificial viral capsids by self-assembly of anionic artificial viral capsid and lipid bilayer containing cationic lipid.